Single Image Super Resolution via Advanced Multiple Mixture Prior model.

Dr.B.Nancharayya, HOD, ECE department, Usha Rama college of engineering and technology, Telaprolu
Mrs.V.Praveena, Associate professor , ECE department, Usha Rama college of engineering and technology, Telaprolu
P.Manusha, 17NG5A0407, ECE department, Usha Rama college of engineering and technology, Telaprolu
P.Vanitha, 16NG1A0445, ECE department, Usha Rama college of engineering and technology, Telaprolu
P.Akhila, 16NG1A0447, ECE department, Usha Rama college of engineering and technology, Telaprolu.

Abstract:

The reconstruction of High Resolution (HR) image from single input Low Resolution (LR) image is main criteria in this paper. Here, we utilize an effective way using mixture prior models to transform the large nonlinear feature space of LR images into a group of linear sub spaces in the training phase. In particular, we first partition image patches into several groups by a novel selective patch processing (SPP) method based on difference curvature of LR patches, and then learning the mixture prior models in each group. Moreover, different prior distributions have various effectiveness in super-resolution, in this case, we find that A-Student-t prior shows stronger performance than the well-known Gaussian prior and student-t prior model. In the testing phase, we adopt the learned multiple mixture prior models to map the input LR features into the appropriate subspace, and finally reconstruct the corresponding HR image in a novel mixed matching way. Experimental results indicate that the proposed approach is both quantitatively and qualitatively superior to some state-of-the-art SR methods.

Index terms—A-Student-t mixture model, Selective patch processing, Difference curvature, Mixed matching.

Introduction:

The main agenda is to reconstruct the visually pleasing HR image from LR image after blurring and down sampling the image. As some researchers the human eye resolution is about 575 Megapixels so that a human can say that the image clear for naked eye or not since the image clarity depends on the devices (like mobile cameras , sensing devices etc.,) used to capture image and storage format's also implicate on the image quality.

Previously there are many SR approaches using basic re sampling kernels or some edge guided approaches to estimate the missing pixel in the HR grid from LR input. The existing interpolation-based approaches are more efficient for real-time SR but in many cases with visual unsatisfactory. Therefore, they are only used for preprocessing LR image rather than the sophisticated SR methods which can recover more details in HR level.

Reconstruction-based methods are developed aiming to reverse the degradation from HR image to LR image by some down-sampling and blurring. They are based on assumptions or prior knowledge about the degradation model. However, this reverse procedure is severely ill-posed as the deficiency of details in the low-resolution inputs. In order to obtain a reliable solution, many regularization methods have been developed to further stabilize the inversion of this ill-posed problem. The most common regularization is the total variation (TV) of the image and its variations. Although these reconstruction-based methods produce sharp edges and suppress aliasing artifacts, they do nothing with sufficient novel details to the HR output, especially at higher magnification.

Before the testing the various training data sets are created to estimate the missing neighboring patch details since the data set is shown in table-1.It shows the comparison of various SR methods with our proposing Advanced student-t MMPM.

	Bicubic			MMPM-S			AMMPM-S		
Images	PSNR	SSIM	IFC	PSNR	SSIM	IFC	PSNR	SSIM	IFC
Butterfly	27.46	0.9145	1.3289	30.64	0.9357	5.6235	42.52	0.9781	7.3759
Child	34.75	0.9791	0.1346	35.56	0.9713	5.0955	39.17	0.9791	5.8493
Coral	26.58	0.9728	0.3276	27.14	0.971	5.1193	40.04	0.9763	5.974
Grains	23.2	0.9796	0.3262	24.05	0.9796	4.758	38.05	0.9755	5.3004
House	26.36	0.9796	0.3821	27.46	0.9797	3.8027	43.85	0.9716	4.2364
Lena	32.79	0.9105	0.4403	35.07	0.9189	5.1639	40.38	0.9749	6.3342
Leopard	29.94	0.9109	0.3667	31.09	0.9133	4.7729	40.08	0.978	5.1315
Louvre	26.36	0.9792	0.3744	27.57	0.9742	5.4027	42.64	0.9714	6.4023
partheneon	28.11	0.9766	0.5191	29.16	0.9796	4.879	42.15	0.9779	5.608
Starfish	30.22	0.9073	0.2305	32.61	0.9182	5.4819	42.48	0.9704	6.7436

Table-1: Comparison table for existing models with our proposed method advanced student-t MMPM.

PSNR -- Peak Signal to Noise Ratio. SSIM -- Structural Similarity Image Measurement. IFC -- Information Fidelity Criteria.

From the Table-1 the Bucolic is the basic SR method and MMPM-S is the existing method our proposed method is far better than the previous methods as shown from the above table PSNR,SSIM,IFC values as PSNR value increases the signal level of information of an image increases then the quality of an image increases.

Framework:

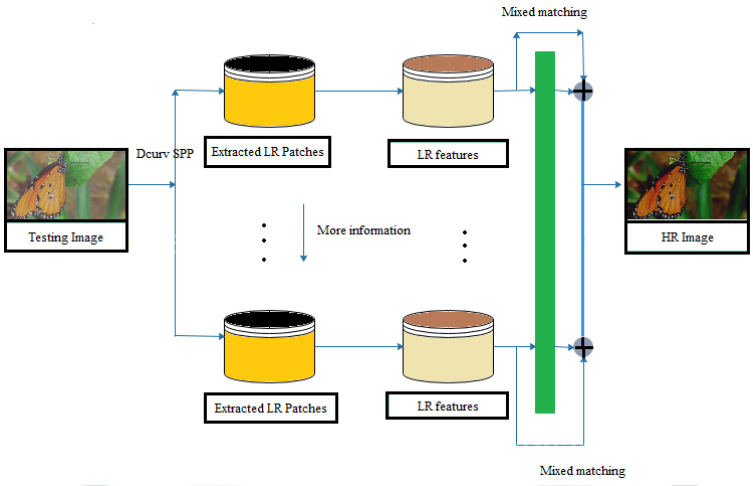

FIG-1: Frame work of the proposed multiple mixture prior model based SR method

The above FIG-1 shows the frame work for the proposed MMPM model. This model main aim is to reduce processing time while maintaining SR reconstruction quality by the mapping relation between LR and HR neighborhood regression SR method. As observed in the above fig the LR image patches and its features are extracted using algorithm Dcurv SPP which is explained detailed later the information was combined by the mixed matching technique which is far better than mono matching technique, then produced the HR image by the collective information.

Algorithm:

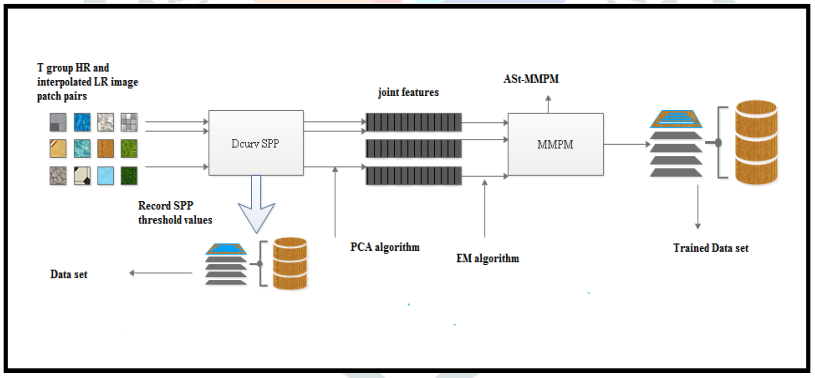

Multiple Mixture prior model base SR has two phases of operation

➢ Training Phase:

Input is taken as N training HR and interpolated LR image patch pairs are taken it is represented as $\{x_i^h, x_i^l\}_{t=1}^N$

Where,

x_i^h, x_i^l Are the images high and low resolution patch information

The numbers of groups are T; number of components in each group is represented as $\{K_t\}_{t=1}^T$, the convergence threshold σ

Output of MMPM is represented as $\{\theta_t\}_{t=1}^T$

To obtain this there are 3 basic operations they are

1. Dcurv-SPP: In this it collect T group of patch pairs $\{x_i^h, x_i^l\}_{t=1}^{Nt}$. And record the SPP thresholds $\{\delta_t\}_{t=1}^{T}$, where. t=1,2,….,T
2. Preparing features: for *t*-to group, extract the joint features $\{x_i\}_{i=1}^{Nt}$ by PCA algorithm and record the PCA as $\{B_t\}_{t=1}^{T}$ where. PCA -- Principle Component Analysis.
3. Leaning mixture prior model: for *t*-th group, apply EM algorithm to learn the mixture prior model as

   i. $\theta_t = \{\nu_k, \omega_k, \mu_k, \sum_k\}_{k=1}^{Kt}$
4. For AStMM: Initialization cluster as $\{x_i\}_{i=1}^{Nt}$ into K_t *partitions* by k-means, value each $\{\nu_k\}_{k=1}^{Kt}$ randomly, $\{\omega_k, \mu_k, \sum_k\}_{k=1}^{Kt}$ are calculated among each partition. and calculated the θ_t using Expectation -Maximization (EM) algorithm.

   - **E-step**: Estimate γ and μ by using Esq.(a),(b)

$$\gamma_{ik} = \frac{\omega_k f_k(x_i)}{\sum_{j=1}^{K} \omega_j f_j(x_i)} ---(a)$$

$$\mu_{ik} = \frac{\nu_k + \eta}{\upsilon_k + (x_i - \mu_k)^T \sum_{ik}^{-1} (x_i - \mu_k)} ----(b)$$

   - **M-step:** calculate θt and μ by using Eqs (c),(d)

$$\omega_k = \frac{1}{N_t} \sum_{i=1}^{N_t} \gamma_{ik} ---(c)$$

$$1 + \frac{1}{\sum_{i=1}^{N_t} \gamma_{ik}} \sum_{i=1}^{N_t} \gamma_{ik} (\log(\mu_{ik}) - \mu_{ik}) - \psi\left(\frac{\nu_k}{2}\right) + \log\left(\frac{\nu_k}{2}\right) + \psi\left(\frac{\nu'_k + \eta}{2}\right) - \log\left(\frac{\nu'_k + \eta}{2}\right) = 0 ----(d)$$

   - Re-evaluate the log-likelihood:

$$L^{iter} = \frac{1}{N} \sum_{i=1}^{N_t} \ln\left[\sum_{k=1}^{K_t} \omega_k f_k(x_i)\right]$$

   To check the convergence

$$\frac{\left|L^{iter} - L^{iter-1}\right|}{L^{iter}} \leq \sigma$$

   If the convergence criterion is not satisfied, update all the parameters and return to the E-step.

➢ Testing Phase :

Input: *M* testing interpolated LR image patches represented as $\{y_i^l\}_{i=1}^{M}$

Learned multiple mixture prior models as $\{\theta_t^T\}_{t=1}^{T}$

SPP thresholds $\{\delta_t\}_{t=1}^{T}$

PCA basis $\{B_t\}_{t=1}^{T}$

Mixed matching level λ

Output: Final SR result.

1. DCurv-SPPand feature extraction: collect *T* groups of LR features $\{y_i^l\}_{i=1}^{Mt}$ according to $\delta_t, t = 1,2,\ldots,T$

2. Select λ appropriate components by sorting the γ' on the models and LR features in each group, which is calculated by Eq.(e) then re-estimate the γ' from γ''

$$k_i = \arg\max \gamma'_{ik} = \arg\max \frac{\omega_k f_k(y_i^l)}{\sum_{j=1}^{K} \omega_j f_j(y_i^l)} ---(e)$$

i.

3. Mixed matching: estimate the expected HR residual features by using Eqs. (f),(g)

i. $$y_{ji}^h = \mu_{kji}^{hl} + \sum_{kji}^{hl} \left(\sum_{kji}^{ll} \right)^{-1} \left(y_i^l - \mu_{kji}^l \right) ---(f)$$

ii. $$y_i^h = \sum_{j=1}^{M} \gamma''_{ij} \, y_{ji}^h ---(g)$$

4. Reconstruction: obtain the HR patches by reshaping HR residual features to patch size and adding the LR patches finally, and then recombine them into a whole HR image.

The proposed multiple mixture prior models (MMPM) based SR method with two phases training and testing, respectively.

In the training phase, we first down-sample each HR training image to mimic the degradation, and then upscale the degraded

LR images to the HR size, where the Bi cubic method is used for these two interpolated procedure. Next, we extract groups of the patch pairs with different degree of informative structures through the proposed difference-curvature based SPP method and record the SPP thresholds, then collect the LR features after using handcraft feature operators and PCA for dimension-reduction and energy-centralization, and concatenate them with the HR residual vectors. Furthermore, an expectation-maximization is applied to learn mixture prior model in each group.

In the testing phase, we first interpolate the input LR testing image to the desired HR size by Bi cubic and extract groups of LR patches under the SPP thresholds, then collect the corresponding features by operation as in the training phase. To be more emphasized, we apply a mixed matching way to reconstruct the HR counterparts and then recombine them into the whole image. For a better view of the proposed SR method, its pseudo code is given in above algorithm.

Experimental Results:

In order to illustrate the superiority of the proposed SR method, we compare its performance with several state-of the-art SR methods, including some prestigious example learning-based SR method: ANR A+ and the well noticed self-example learning method as Self ExSR .In the field of deep learning, SR is also a conspicuous branch, which has boost several high-efficiency SR methods, such as SRCNN and FSRCNN-s are also concerned to be competitors in this section. To be comparable, all the experiments are conducted on the available Mat-lab (R2018a) codes under the same experimental environment with an Intel core i3 CPU and 8GB of memory. Moreover, the results are far better in the i7 processor with 16GB of memory .For color images, we first transform the RGB images into YCbCr format. Since human are more sensitive to the luminance changes in color images, only the luminance channel is evaluated through the proposed method. The simulation model in mat-lab is represented in the fig-3.

The experiment is performed on several images and they are shown in following images the experiment results are shown with three main basics they are first image represents the SR input image which is blurred then second image is HR image which is resized to HR range then the third image is AStMMPM applied on the resized image then zoom a particular portion by the scale factor of $\times 2, \times 3, \times 4$ respectively. The extension represents the advanced student-t mixture prior model since the values are extended to the previous version of student-t mixture prior model as shown in the table-1.

Followed by the result images the values are also shown below individually in a tabular form by presenting the PSNR,SSIM,IFC values for each image on the results.

From FIG-4 to F-13 representing the result details clearly.

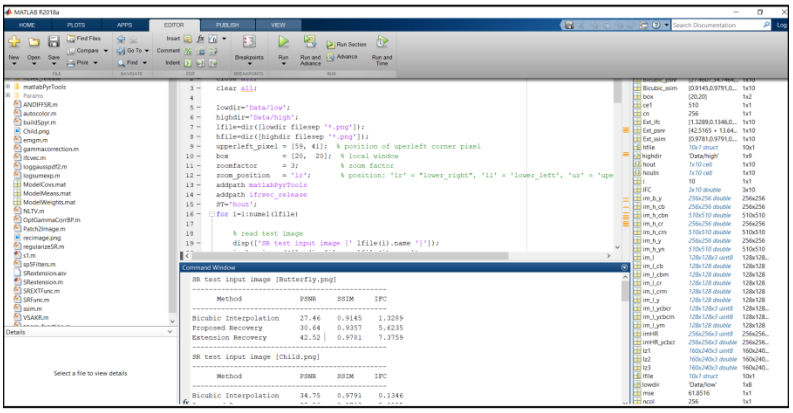

FIG:3 simulation model using matlabR2018a

SR test input image [Butterfly.png]

Method	PSNR	SSIM	IFC
Bicubic Interpolation	27.46	0.9145	1.3289
Proposed Recovery	30.64	0.9357	5.6235
Extension Recovery	42.52	0.9781	7.3759

FIG:4 Butterfly SR output images with their PSNR , SSIM , IFC values with *3 scale factor

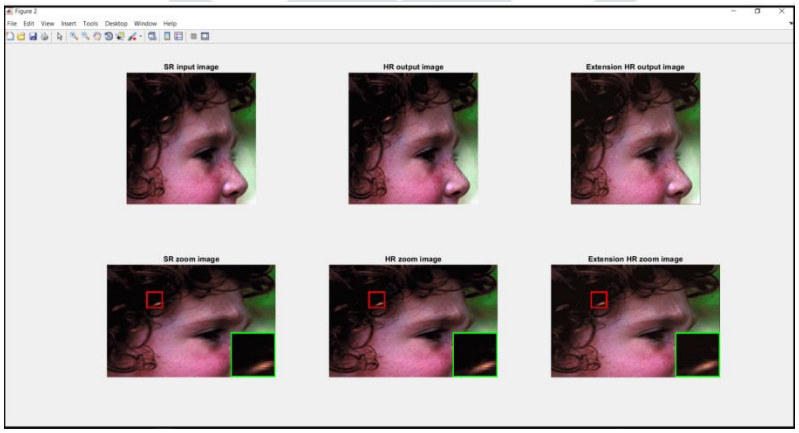

```
-----------------------------------------------
SR test input image [Child.png]
-----------------------------------------------
      Method                PSNR      SSIM      IFC
-----------------------------------------------
Bicubic Interpolation       34.75     0.9791     0.1346
Proposed Recovery           35.56     0.9713     5.0955
Extension Recovery          39.17     0.9791     5.8493
-----------------------------------------------
```

FIG: 5 Child SR output images with their PSNR, SSIM, IFC values with *3 scale factor

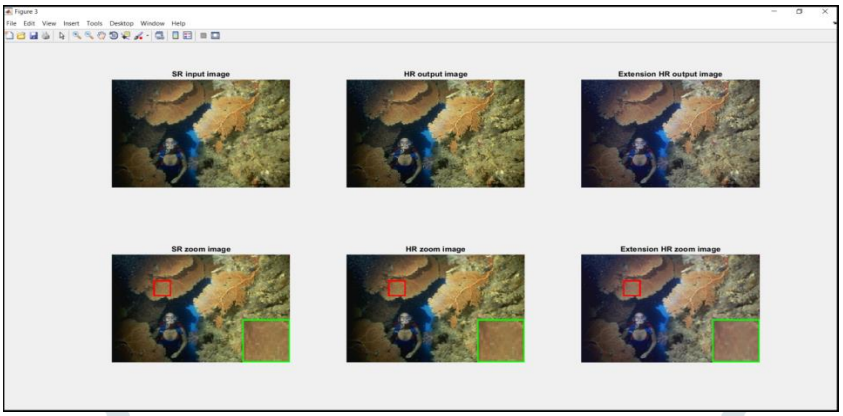


```
-----------------------------------------------
SR test input image [Coral.png]
-----------------------------------------------
      Method                PSNR      SSIM      IFC
-----------------------------------------------
Bicubic Interpolation       26.58     0.9728     0.3276
Proposed Recovery           27.14     0.9710     5.1193
Extension Recovery          40.04     0.9763     5.9740
-----------------------------------------------
```

FIG:6 Coral SR output images with their PSNR , SSIM , IFC values with *3 scale factor

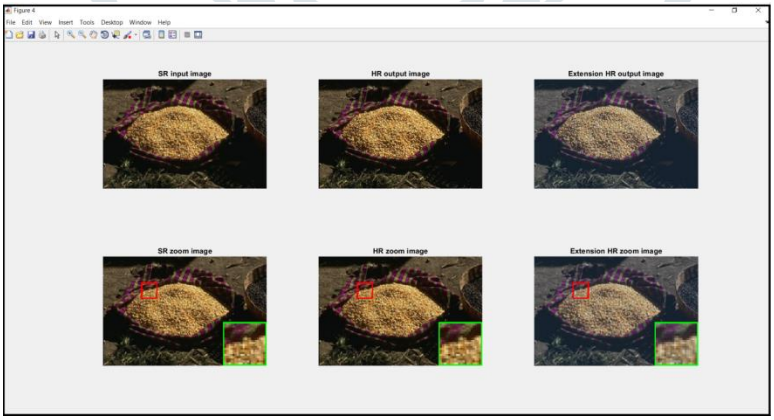


```
-----------------------------------------------
SR test input image [Grains.png]
-----------------------------------------------
      Method                PSNR      SSIM      IFC
-----------------------------------------------
Bicubic Interpolation       23.20     0.9796     0.3262
Proposed Recovery           24.05     0.9796     4.7580
Extension Recovery          38.05     0.9755     5.3004
-----------------------------------------------
```

FIG:7 Grains SR output images with their PSNR , SSIM , IFC values with *3 scale factor

SR test input image [House.png]

Method	PSNR	SSIM	IFC
Bicubic Interpolation	26.36	0.9796	0.3821
Proposed Recovery	27.46	0.9797	3.8027
Extension Recovery	43.85	0.9716	4.2364

FIG:8 House SR output images with their PSNR , SSIM , IFC values with *3 scale factor

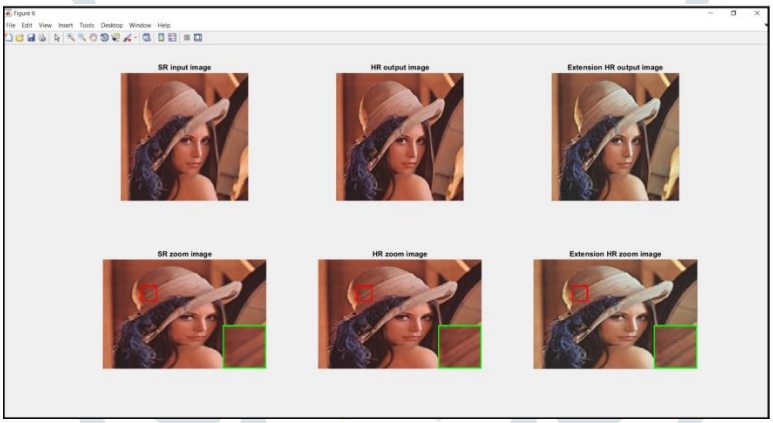

SR test input image [Lena.png]

Method	PSNR	SSIM	IFC
Bicubic Interpolation	32.79	0.9105	0.4403
Proposed Recovery	35.07	0.9189	5.1639
Extension Recovery	40.38	0.9749	6.3342

FIG:9 Lena SR output images with their PSNR , SSIM , IFC values with *3 scale factor

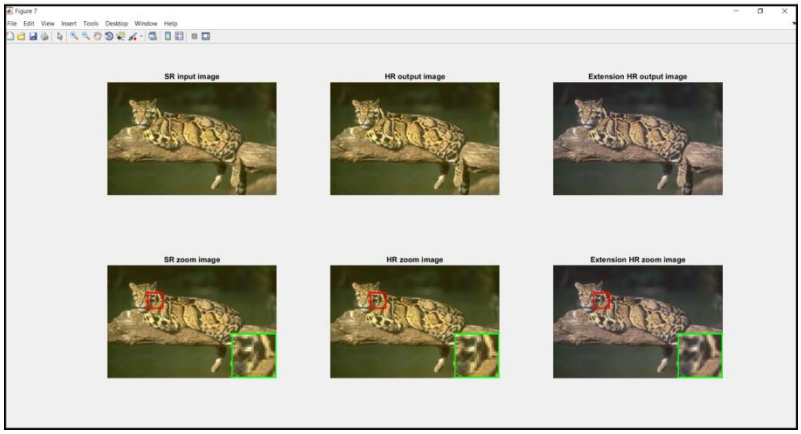

SR test input image [Leopard.png]

Method	PSNR	SSIM	IFC
Bicubic Interpolation	29.94	0.9109	0.3667
Proposed Recovery	31.09	0.9133	4.7729
Extension Recovery	40.08	0.9780	5.1315

FIG:10 Leopard SR output images with their PSNR , SSIM , IFC values with *3 scale factor

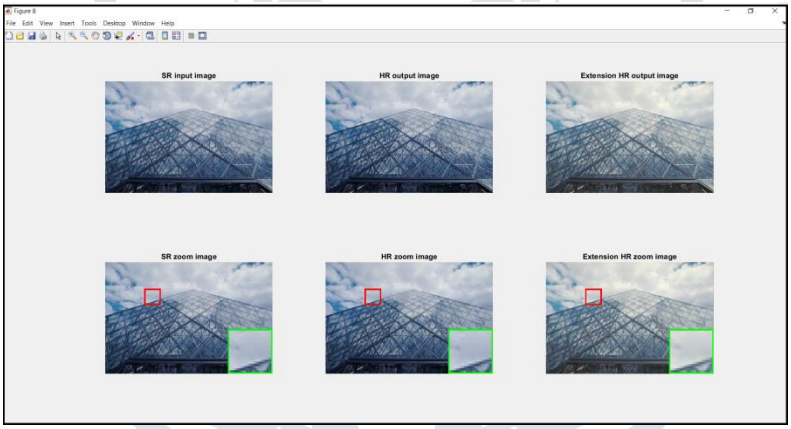

SR test input image [Louvre.png]

Method	PSNR	SSIM	IFC
Bicubic Interpolation	26.36	0.9792	0.3744
Proposed Recovery	27.57	0.9742	5.4027
Extension Recovery	42.64	0.9714	6.4023

FIG:11 Louvre SR output images with their PSNR , SSIM , IFC values with *3 scale factor

SR test input image [Partheneon.png]

Method	PSNR	SSIM	IFC
Bicubic Interpolation	28.11	0.9766	0.5191
Proposed Recovery	29.16	0.9796	4.8790
Extension Recovery	42.15	0.9779	5.6080

FIG: 12 Parthenon SR output images with their PSNR , SSIM , IFC values with *3 scale factor

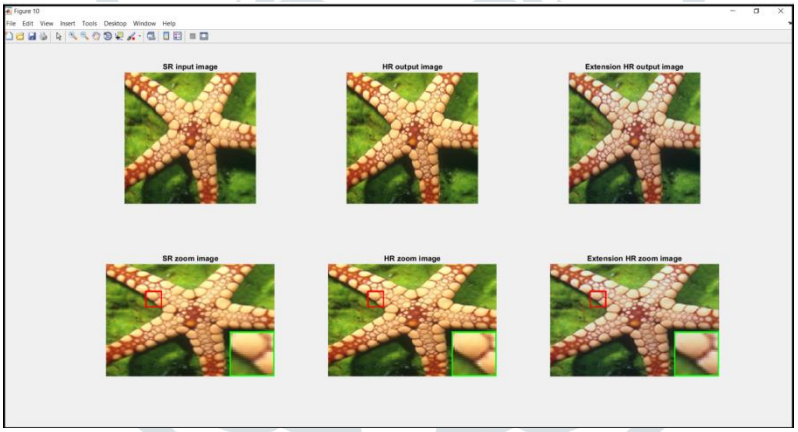

SR test input image [Starfish.png]

Method	PSNR	SSIM	IFC
Bicubic Interpolation	30.22	0.9073	0.2305
Proposed Recovery	32.61	0.9182	5.4819
Extension Recovery	42.48	0.9704	6.7436

FIG: 13 Starfish SR output images with their PSNR, SSIM , IFC values with *3 scale factor


```
-----------------------------------------------
SR test input image [manuimage.png]
-----------------------------------------------
      Method                PSNR      SSIM      IFC
-----------------------------------------------
Bicubic Interpolation      32.34     0.9359     0.2512
Proposed Recovery          33.71     0.9350     3.8811
Extension Recovery         45.95     0.9749     4.0553
-----------------------------------------------
```

FIG: 14 Real time SR manuimage (128-LR)(256-HR)with their PSNR , SSIM , IFC values with *3 scale factor

Conclusion:

Hence we perform experiment on the i3 processor it is far better output compared to the previous one also we successfully performed this experiment on real time images by maintaining their standard size at both LOW and HIGH images. The results are presented in this paper with the values we mostly recommend this experiment should be done on i7 processor with 16GB memory because most of the image processing has an drawback that compared to GPU(Graphical Processing Unit) CPU lacks some operations since it also takes more time to execute the required data. In this paper we fully focus on the MMPM (Multiple Mixture Prior Models) and we proposing the advanced student-t multiple mixture prior model which improve the PSNR value and it reduces the execution time.

References:

1. R. Keys, “Cubic convolution interpolation for digital image processing,” IEEE Transactions on Acoustics, Speech, and Signal Process., vol. 29, no. 6, pp. 1153–1160, Dec. 1981.
2. X. Li and M. T. Orchard, “New edge-directed interpolation,”IEEE Trans. Image Process., vol. 10, no. 10, pp. 1521–1527, Oct. 2001.
3. L. Zhang and X. Wu, “An edge-guided image interpolation algorithm via directional fifiltering and data fusion,”IEEE Trans. Image Process., vol. 15, no. 8, pp. 2226–2238, Aug. 2006.
4. R. Fattal, “Image upsampling via imposed edge statistics,” ACM Trans. Graph., vol. 26, no. 3, pp. 95–1–95–8, Jul. 2007.
5. L. I. Rudin, S. Osher, and E. Fatemi, “Nonlinear total variation based noise removal algorithms,” Physica D: Nonlinear Phenomena, vol. 60, no. 1, pp. 259–268, Nov. 1992.
6. A. Marquina and S. Osher, “Image super-resolution by tv-regularization and bregman iteration,” J. Sci. Comput., vol. 37, no. 3, pp. 367–382, Dec. 2008.
7. W. Dong, L. Zhang, G. Shi, and X. Wu, “Image deblurring and superresolution by adaptive sparse domain selection and adaptive regularization,”IEEE Trans. Image Process., vol. 20, no. 7, pp. 1838–1857, Jul. 2011.
8. Q. Yuan, L. Zhang, and H. Shen, “Multiframe super-resolution employing a spatially weighted total variation model,”*IEEE Trans.* Circuits Syst. Video Technol., vol. 22, no. 3, pp. 379–392, Mar. 2012.
9. Q. Yuan, L. Zhang, and H. Shen, “Regional spatially adaptive total variation super-resolution with spatial information filtering and clustering,”IEEE Trans. Image Process., vol. 22, no. 6, pp. 2327–2342, Jun. 2013.
10. C. Fernandez-Granda and E. J. Candes, “Super-resolution via transform- ` invariant group-sparse regularization,” in Proc. IEEE *Int.* Conf. Comput. Vis. (ICCV), Dec. 2013, pp. 3336–3343.
11. C. Ren, X. He, and T. Q. Nguyen, “Single image super-resolution via adaptive high-dimensional non-local total variation and adaptive geometric feature,” IEEE Trans. Image Process., vol. 26, no. 1, pp. 90– 106, Jan. 2017.

12. J. Yang, J. Wright, T. Huang, and Y. Ma, "Image super-resolution as sparse representation of raw image patches," in Proc. IEEE Conf. Comput. Vis. Pattern Recognit. (CVPR*)*, Jun. 2008, pp. 1–8.
13. J. Yang, J. Wright, T. S. Huang, and Y. Ma, "Image super-resolution via sparse representation,"IEEE Trans. Image Process., vol. 19, no. 11, pp. 2861–2873, Nov. 2010.
14. J. Yang, Z. Wang, Z. Lin, S. Cohen, and T. Huang, "Coupled dictionary training for image super-resolution," IEEE Trans. Image Process., vol. 21, no. 8, pp. 3467–3478, Aug. 2012.
15. R. Zeyde, M. Elad, and M. Protter, "On single image scale-up using sparse-representations," in Proc. Int. Conf. Curves Surfaces, Jun. 2010, pp. 711–730.
16. R. Timofte, V. De, and L. V. Gool, "Anchored neighborhood regression for fast example-based super-resolution," in Proc. IEEE Int. Conf. Comput. Vis. (ICCV), Dec. 2013, pp. 1920–1927.
17. R. Timofte, V. De, and L. V. Gool, "A+: Adjusted anchored neighborhood regression for fast super-resolution," in Proc. 12th Asian Conf. Comput. Vis. (ACCV), Nov. 2014, pp. 111–126.
18. R. Timofte, R. Rothe, and L. V. Gool, "Seven ways to improve example based single image super resolution," in *Proc.* IEEE Conf.Comput. Vis. Pattern Recognit. (CVPR*)*, Jun. 2016, pp. 1865–1873.
19. K. Zhang, D. Tao, X. Gao, X. Li, and Z. Xiong, "Learning multiple linear mappings for effificient single image super-resolution," IEEE Trans. Image Process., vol. 24, no. 3, pp. 846–861, Mar. 2015.
20. K. Zhang, D. Tao, X. Gao, X. Li, and J. Li, "Coarse-to-fifine learning for single-image super-resolution," IEEE Trans. Neural Netw. Learn. Syst., vol. 28, no. 5, pp. 1109–1122, May. 2017.